The multiple V-shaped double peeling of elastic thin films from elastic soft substrates

N. Menga [a], L. Afferrante [a,*], N.M. Pugno [b,c,d], G. Carbone [a,e,f]

[a] *Department of Mechanics, Mathematics and Management, Politecnico of Bari, V.le Japigia, 182, 70126 Bari, Italy*
[b] *Laboratory of Bio-Inspired and Graphene Nanomechanics, Department of Civil, Environmental and Mechanical Engineering, University of Trento, Via Mesiano 77, 38123 Trento, Italy*
[c] *School of Engineering and Materials Science, Queen Mary University of London, Mile End Road, London E1 4NS, United Kingdom*
[d] *Ket Lab, Edoardo Amaldi Foundation, Italian Space Agency, Via del Politecnico snc, 00133 Rome, Italy*
[e] *Physics Department, "M. Merlin", CNR - Institute for Photonics and Nanotechnologies U.O.S., via Amendola 173, 70126 Bari, Italy*
[f] *Department of Mechanical Engineering, Imperial College London, Exhibition Road, London SW7 2AZ, United Kingdom*

ARTICLE INFO

ABSTRACT

In this paper, a periodic configuration of V-shaped double peeling process is investigated. Specifically, an elastic thin film is detached from a soft elastic material by applying multiple concentrated loads periodically distributed with spatial periodicity λ. The original Kendall's idea is extended to take into account the change in elastic energy occurring in the substrate when the detachment fronts propagate. The symmetric configuration typical of a V-peeling process causes the energy release rate to be sensitive to variations of the elastic energy stored in the soft substrate. This results in an enhancement of the adhesion strength because part of the external work required to trigger the peeling mechanism is converted in substrate elastic energy.

A key role is played by both spatial periodicity λ and elasticity ratio E/E_h, between tape and substrate elastic moduli, in determining the conditions of stable adhesion. Indeed, the presence of multiple peeling fronts determines a modification of the mechanism of interaction, because deformations close to each peeling front are also affected by the stresses related to the other fronts. Results show that the energy release rate depends on the detached length of the tape so that conditions can be established which lead to an increase of the supported load compared to the classical peeling on rigid substrates.

Finally, we also find that for any given value of the load per unit length, an optimum value of the wavelength λ exists that maximizes the tolerance of the system, before unstable propagation of the peeling front can occur.

© 2018 Elsevier Ltd. All rights reserved.

1. Introduction

In the last decades, biological and biomechanical applications have boosted the interest in the adhesive contact of thin films, making it an important topic in contact mechanics (Afferrante and Carbone, 2013; Carbone et al., 2011; Dening et al., 2014; Ding et al., 2001; Jin, 2009; Menga et al., 2016a; Pesika et al., 2007; Pugno, 2011; Shanahan, 2000; Varenberg et al.,

---

* Corresponding author.
  E-mail address: luciano.afferrante@poliba.it (L. Afferrante).

2010; Wan, 2001). In nature, several organisms show enhanced adhesion thanks to hierarchical structures of hairs or setae. For instance, hairy attachment systems of insects, arachnids and reptiles have been intensively studied during the past years, aiming at explaining and possibly mimic their extraordinary adhesive abilities in artificial bio-mimetic devices (Afferrante and Carbone, 2012; Afferrante et al., 2015; Carbone and Pierro, 2012a,b; Geim et al., 2003; Glassmaker et al., 2007; Gravish et al., 2008; Krahn et al., 2011; Murphy et al., 2011; Pugno, 2008).

To this regard, several studies have been devoted to soft elastic contacts in presence of adhesion (Carbone and Mangialardi, 2008; Hui et al., 2001; Menga et al., 2016a, 2018; Persson, 2003), and specifically to the detachment process (del Campo et al., 2007; Lee et al., 2008; Sekiguchi et al., 2015). Experimental observations of insects and spiders (Autumn et al., 2006b; Autumn and Peattie, 2002; Huber et al., 2005) and theoretical studies (O'Rorke et al., 2016; Ozer, 2016; Varenberg and Gorb, 2007) have made clear the crucial role played by highly flexible terminal spatula-shaped substructures attached to their legs, which finally allows them to easily climb on surfaces with different properties in terms of roughness and compliance.

The role of roughness is not yet completely understood. Several theoretical (Carbone and Mangialardi, 2004; Guduru, 2007; Persson, 2002), numerical (Carbone and Mangialardi, 2008; Carbone et al., 2016; Ciavarella et al., 2017; Wu, 2012) and experimental (Dies et al., 2015; Guduru and Bull, 2007; Martina et al., 2012a,b) studies have shown that high surface roughness reduces interfacial adhesion. However, some insects, like geckos, are able to achieve extremely high adhesive performance also on rough substrates. Some models have been proposed which attempt to explain this interesting behavior (Arzt et al., 2003; Huber et al., 2005; Persson, 2003; Pesika et al., 2007; Tian et al., 2006). For instance, in Ref. Tian et al. (2006), it is shown that high adhesion forces are obtained by rolling down and inward the toes to realize small peeling angle during the attachment. Detachment is instead obtained by rolling the toes upward and backward. Also, the gecko ability to remain stuck while inverted on the ceiling has been investigated in Refs. (Autumn et al., 2006a; Lepore et al., 2012). Those studies show that geckos use opposing feet and toes to prevent detachment of setae or peeling of toes.

Therefore, since the 50's, several studies have been devoted to understand the mechanism governing peeling (Barquins and Ciccotti, 1997; Kaelble, 1959, 1965; Kendall, 1975). Interest in practical applications, such as defining specific peeling tests standards to characterize the adhesive properties of joints involving thin films (ISO 8510-1, 1990; ISO 8510-2, 2006), has led researchers to focus on phenomena involved in peeling process. In this respect, a very comprehensive review is provided in Ref. (Creton and Ciccotti, 2016). About phenomena occurring at interface, several works have investigated the intrinsic bi-layered nature of typical commercial tapes (e.g. 3M Scotch), where the adhesive soft layer is backed to a thin stiffer one. In this case, during the peeling process a loss of confinement of the soft adhesive part gives rise to generation of a macroscopic debonding region characterized by fibrillar adhesive bridges and progressive bending deformation of the tape (Callies et al., 2016; Villey et al., 2017, 2015). It is also interesting to recall that when the adhering surfaces are rough, air pockets can remain trapped at the interface, depending on the material properties, the strength of adhesive interactions, and the topography of the surface (see, for example, Refs. (Creton and Leibler, 1996; Hui et al., 2000; Persson et al., 2004)). Moreover, in some cases, as the peeling process advances and the interface between the layers is interested by tensile stress, high speed camera images (see Ref. Lakrout et al., 1999) show nucleation and growth of cavities, near to the peak stress region, which make the layers deformation no longer homogeneous.

Such studies typically rely on the assumption of compliant films on rigid substrates. For a large class of practical applications, this hypothesis leads to physically realistic results. However, there exist several other applications, where a more proper formalism is required to take into account the effect of the substrate compliance on the detachment mechanism, as for instance studying the adhesive contact of medical Band-aids on human skin (Chivers, 2001; Kwak et al., 2011). In this case, indeed, the deformability of the substrate have to be taken into account, and although the skin is usually modeled as a very compliant viscoelastic material (Boyer et al., 2007; Edwards and Marks, 1995; Pereira et al., 1991; Silver et al., 2001), interesting results may be inferred neglecting viscous effects at low speeds, because in such case the behavior is essentially elastic (Menga et al., 2014, 2016b, 2017).

Moreover, dealing with deformable substrates, the specific geometrical configuration of the peeling system strongly affects the process evolution. As reported in Refs. (Bosia et al., 2014; Pugno, 2011; Wolff et al., 2015), specific patterns of multiple and opposite peeling fronts can be recognized in the detachment process of gecko's toes as well as in proximity of spider webs anchors (see Fig. 1). In these systems, the interaction between the elastic fields, generated by the multiple peeling fronts, plays a key role in determining the detachment behavior. Indeed, differently from the classical Kendall's peeling, where the mechanism of detachment is unaffected by the elastic properties of the substrate (Afferrante and Carbone, 2016; Kendall, 1975), in the V-shaped double peeling case translation invariance is lost. Consequently, as the peeling front advances, variation in the elastic energy stored in the substrate cannot be neglected. This entails a change in the external work required to trigger the detachment process, which in turn modifies the peeling mechanism.

We stress that for the first time it is made clear that the combined effect of considering a V-shaped peeling configuration (which causes the loss of translation invariance) and a compliant substrate (which enables interaction between the elastic displacements fields associated with the peeling fronts) results in an enhancement of the adhesion strength.

2. Formulation

Consider the symmetric V-shaped periodic double peeling scheme shown in Fig. 2. The system is constituted by an elastic thin film of thickness d, and transversal width b, adhering to a linear elastic half-plane. The film is assumed infinitely
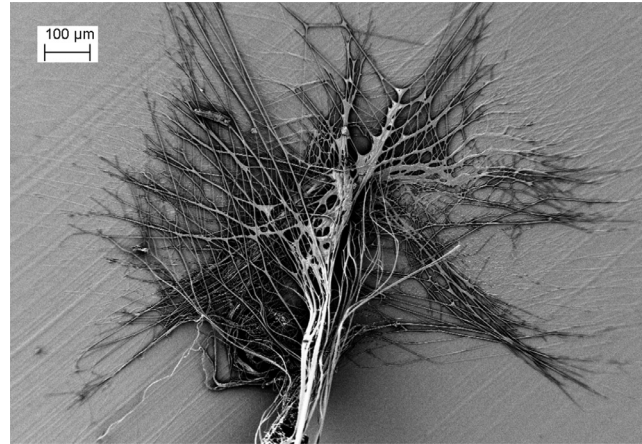
Fig. 1. A Scanning electron microscope image of a spider web anchor. Multiple V-shaped attachment points can be seen.
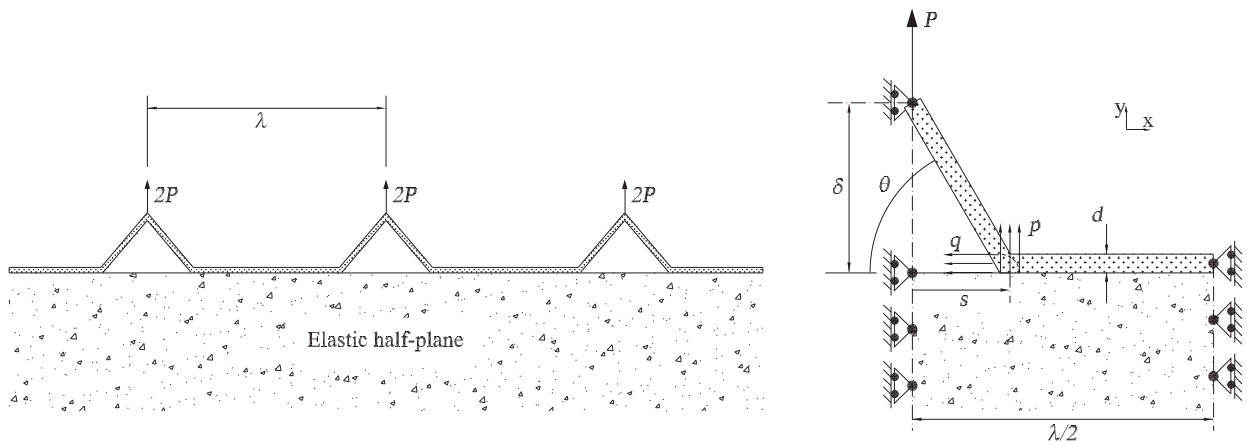

Fig. 2. The periodic V-shaped double peeling scheme. Periodicity and symmetry of the problem can be exploited to focus the study on half of a single elementary cell.

flexible, and is peeled off by applying multiple vertical forces $2P$ periodically distributed with spatial periodicity λ. Under the assumption of linearity and small deformations, physical arguments (see Ref. Afferrante and Carbone, 2016) suggest that the overall load $T = P/(\sin\theta)$ distributes in proximity of the detachment front over a strip of length $2a$ of the same order of d. Consequently, the surface displacements of the elastic substrate can be calculated with good accuracy by considering two uniform distributions of normal $p_n(x) = p = P/(2ab)$ and tangential $p_t(x) = q = -P\cot\theta/(2ab)$ tractions, acting on a strip of size $2a \simeq \alpha d$, where α is a proportionality constant expected to be of the order of the unity; thus for the following numerical examples we have fixed $\alpha = 1$. With reference to normal stresses, such assumption is indeed confirmed in Ref. (Kaelble, 1960); about shear stresses, one can easily show that they are necessarily distributed on a region of size proportional to $(E/E_h)^{1/2}\sqrt{\lambda d}$, being E and E_h the elastic moduli of the thin film and half-plane, respectively. However, though our assumption about the extension of the region of distribution of tangential tractions may be a bit stronger in some cases, we expect it does not modify qualitatively the main physical scenario.

The symmetry typical of a double V-peeling configuration entails the loss of translation invariance, and makes the calculation of the energy release rate sensitive to the variation of the elastic energy in the substrate during the peeling fronts propagation. Such energy variation is also affected by the interaction between the peeling fronts, as deformations close to a peeling front also depend on the stresses related to the other fronts. In particular, with reference to Fig. 2 in order to calculate the surface displacements of the substrate, two mechanisms of interaction need to be considered. The first one is related to the fronts belonging to the same V-peel, and is taken into account by superposing the displacements due to each single peeling front: $\mathbf{u_{tot}}(s,x) = \mathbf{u}(x-s) + \mathbf{u}(x+s)$, being s the detached length. The latter is related to the periodic adjacent V-peels, and is intrinsically considered by calculating the displacements vector $\mathbf{u} = (u_x, u_y)$, due to the periodic surface tractions q and p, by means of the Green's functions given in appendix A.

In presence of very soft materials, large deformations might magnify the effects of interaction between peeling fronts, but would not modify the main physics governing the considered problem, i.e. the qualitative behavior of the peeling process

would not be affected by the presence of large deformations. Indeed, under the JKR assumption (Johnson et al., 1971), large deformations and material nonlinearity have small effects on the adhesion of soft elastic materials (see, for example, Ref. Lin and Chen, 2006).

In the framework of the above assumptions, it is straightforward demonstrating that the tape continuity equation writes as

$$\delta \sin \theta = s(1 - \cos \theta + \varepsilon), \tag{1}$$

where $\delta \sin \theta$ is the component of the displacement of the point of application of P along the tape direction and $\varepsilon = (dl' - dl)/dl = P/(Ebd \sin \theta)$ is the elongation of the tape per unit length, being E the Young's modulus of the tape material. Furthermore, from simple geometrical considerations we can also write

$$s(1 + \varepsilon) \cos \theta = s \qquad \rightarrow \qquad \left(1 + \frac{P}{Ebd \sin \theta}\right) \cos \theta = 1 \tag{2}$$

which defines a one to one relation between the applied force P and the peeling angle θ. Moreover, to completely define the problem we need to find the equilibrium condition. For a reversible and isothermal transformation, the system spontaneously moves out of equilibrium when the variation of the total energy is negative, i.e.

$$dU_{tot} = dU_{el,t} + dU_{el,h} + dU_P + dU_{ad} < 0, \tag{3}$$

where $dU_{el,t}$ and $dU_{el,h}$ are, respectively, the change in the elastic energy stored in the tape and substrate, dU_P is the variation of the potential energy associated with the applied peeling force P and dU_{ad} is the change in the surface energy. The surface adhesion energy is $U_{ad} = \Delta \gamma bs$, being $\Delta \gamma$ the Duprè energy of adhesion, whereas the elastic strain energy stored in the tape can be calculated as $U_{el,t} = T^2 s/(2Ebd)$. Considering that the bending stiffness of the tape depends on the cubic power of the thickness d, the contribution of bending in terms of change of elastic energy during peeling propagation is negligible, as indeed observed in Ref. Villey et al., 2017. The elastic energy stored in the half-plane is

$$U_{el,h} = \frac{1}{2} b \int_{s-d/2}^{s+d/2} \sigma \cdot \mathbf{u}_{tot}(s, x) dx, \tag{4}$$

where $\sigma = (q, \; p)$ is the vector of the normal and tangential tractions. The potential energy is instead $U_P = -Pu_P$, where u_P is the total vertical displacement of the point of application of P

$$u_P = u_{y,tot}(s, s) + \delta = u_{y,tot}(s, s) + s \tan \theta \tag{5}$$

Recalling that the energy release rate G on the peeling front is defined as (Ref. Maugis and Barquins, 1988)

$$G = -\frac{\partial (U_{tot} - U_{ad})}{\partial A} = -\frac{1}{b} \left(\frac{\partial U_{el,t}}{\partial s} + \frac{\partial U_{el,h}}{\partial s} + \frac{\partial U_P}{\partial s} \right) \tag{6}$$

Eq. (3) can be rewritten as

$$dU_{tot} = -(G - \Delta \gamma) bds < 0 \tag{7}$$

Therefore, if $G > \Delta \gamma$ the above inequality requires $ds > 0$ and the crack will spontaneously advance causing the detachment of the tape; if $G < \Delta \gamma$, then $ds < 0$ and peeling is prevented. As a result, the equilibrium condition can be obtained by enforcing $G = \Delta \gamma$. The above formulation has been obtained under the assumption of negligible inertia effects. As a consequence, our results are expected to be physically sound for peeling velocities sufficiently smaller than the characteristic propagation speed of waves in the material. Under dynamic conditions, both experimental and numerical investigations (Barquins and Ciccotti, 1997; Ciccotti et al., 2004; Rumi and Ananthakrishna, 2006) show the occurrence of dynamic instabilities, which cannot be captured with the present model. In such a case, in particular, the calculation of the energy release rate should also take into account the kinetic energy contribution (Dalbe et al., 2014a,b).

3. Results

Results are given for substrate of incompressible material (Poisson's ratio $\nu_h = 0.5$).

Fig. 3 shows, in a semi-log plot, the dimensionless energy release rate $\hat{G} = G/(Ed)$ as a function of the dimensionless detached length $\hat{s} = s/d$, at different applied loads, for rigid (3a) and compliant (3b) substrate, respectively. The dimensionless work of adhesion $\Delta \hat{\gamma} = \Delta \gamma/(Ed)$ is plotted with red dashed line. In particular, in Fig. 3a, the solution given in Afferrante et al. (2013); Putignano et al. (2014) is plotted for tape initially fully stuck to the substrate ($h \rightarrow 0$, being h a length of the tape initially not attached). When the substrate is rigid, $\hat{G}$ is not affected by the detached length. Moreover, peeling is prevented when $P/P_0 < 1$ and unstable detachment always occurs for $P/P_0 > 1$, being P_0 the load value for which $\hat{G} = \Delta \hat{\gamma}$. Notice $P_0 = T_0 \sin \theta$, where T_0 corresponds to the Kendall's critical load, which can be obtained by solving

$$\frac{T_0}{b} \left(1 - \cos \theta + \frac{T_0}{Ebd} \right) = \Delta \gamma \tag{8}$$

A different behavior is observed in Fig. 3b for compliant substrate. First, $\hat{G}$ monotonically increases with $\hat{s}$. Therefore, stable adhesion is possible *even* for $P/P_0 > 1$ provided the detached length s is lower than a threshold value $s_{th}(P)$, which
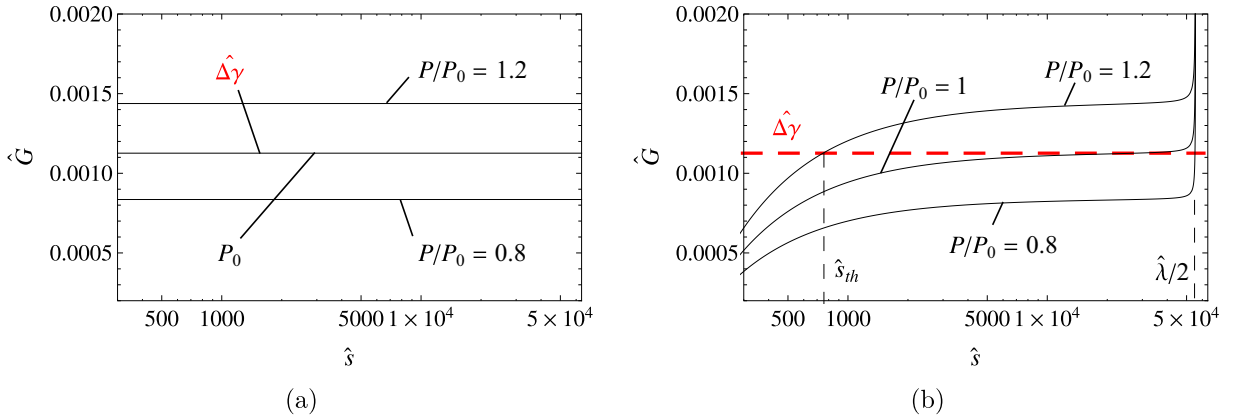
Fig. 3. The dimensionless energy release rate $\hat{G}$ as a function of the dimensionless detached length $\hat{s}$, for different applied loads P/P_0 on rigid (a) and compliant (b) substrate, respectively. The value of the dimensionless work of adhesion $\Delta\hat{\gamma} = 1.126$ is plotted with red dashed line. Results are obtained for $\chi = E/E_h = 500$ and $\lambda/d = 10^5$. The values on x-axis are given in log scale. (For interpretation of the references to colour in this figure legend, the reader is referred to the web version of this article.)
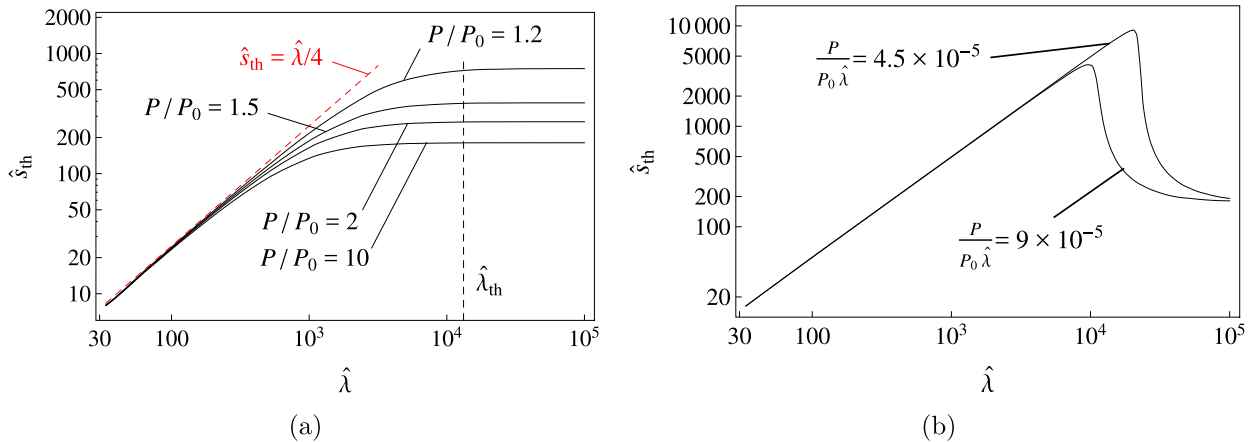
Fig. 4. The dimensionless threshold value $\hat{s}_{th}$ of the detached length as a function of the dimensionless load pitch $\hat{\lambda}$ (a) for different applied loads, (b) for different loads per unit length. Results are given for $\chi = E/E_h = 1000$ and $\Delta\hat{\gamma} = 1.126$.

depends on the load P. Above s_{th}, G becomes larger than $\Delta\gamma$, and unstable propagation of the peeling front is expected to occur.

According to the Griffith's criterion, equilibrium occurs at the point $\hat{G} = \Delta\hat{\gamma}$. However, such point of equilibrium is unstable. In fact, $\Delta\gamma$ represents the work required to advance the detachment front by one unit length, and G the energy available for the peeling front propagation. Therefore, starting from the equilibrium, a small increment of the detached length involves $G > \Delta\gamma$, i.e. there is more released energy than the adhesion energy gained by separating the surface, leading to peeling propagation instability. Fig. 3b also shows that for a periodic V-shaped peeling, the tape can sustain loads larger than P_0 provided that $s < s_{th}(P)$.

Fig. 4a shows the dimensionless threshold value $\hat{s}_{th} = s_{th}/d$ of the detached length as a function of the dimensionless spatial periodicity $\hat{\lambda} = \lambda/d$, for different applied loads. We note that, almost independently of the applied load, the quantity s_{th} is proportional to the spatial periodicity λ (provided that λ is not too large) taking the value $s_{th} = \lambda/4$, which corresponds to a distance between the two peeling fronts just equals half the spatial periodicity, i.e. to a configuration where all the peeling fronts are equi-spaced. On the other hand for sufficiently large value of λ the threshold value s_{th} reaches a plateau, which instead significantly depends on the applied load P.

Further, interesting conclusions can be drawn from Fig. 4b, where, this time, the relation between $\hat{s}_{th}$ and $\hat{\lambda}$ is investigated at fixed load per unit length. Specifically, s_{th} linearly increases with λ up to a critical value beyond which a strong reduction is observed. This behavior, peculiar of periodic V-shaped double peeling processes, is of straightforward interest for engineering applications, entailing the possibility to arrange the contacts with the specific spatial periodicity λ that, given the size of the initial defect (i.e., the initial detached length), maximizes the peeling load per unit length.
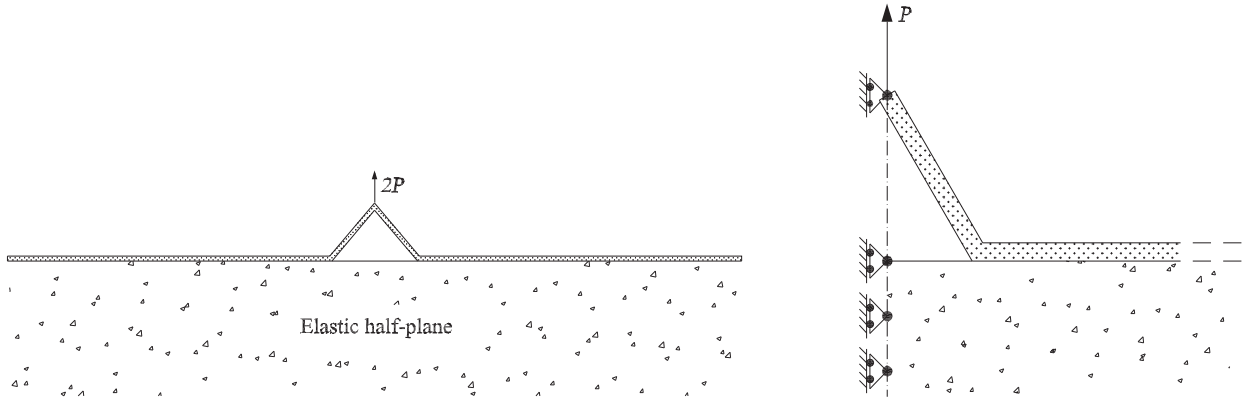
Fig. 5. The scheme of single V-shaped double peeling of an elastic thin film from a compliant elastic substrate.
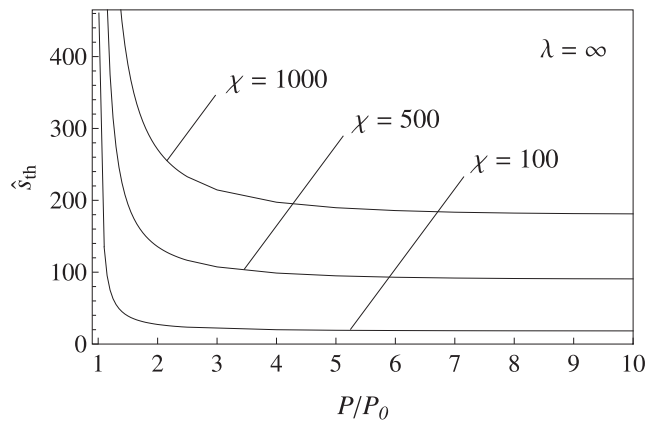

Fig. 6. The dimensionless threshold of the detached length $\hat{s}_{th}$ as a function of the normalized peeling load P/P_0 for different values of the elasticity ratio $\chi = E/E_h$. The regions under the curves correspond to stable and safe states of adhesion. Above the curves unstable detachment is expected.

3.1. The asymptotic limit $\lambda \to \infty$

In the limit of large values of λ, the asymptotic *aperiodic* behavior corresponding to the geometric scheme of Fig. 5 is recovered.

For this case, Fig. 6 shows the variation of the threshold $\hat{s}_{th}$ with the peeling load P, normalized with respect to P_0, for different values of the elasticity ratio $\chi = E/E_h$ between the tape and half-space elastic moduli.

Increasing P/P_0 leads to an initial sharp reduction in $\hat{s}_{th}$, which then converges to a limiting value at high loads. In particular, if the elasticity ratio χ is not too large, for loads P just exceeding P_0, the threshold $\hat{s}_{th}$ takes small values and adhesion can be guaranteed only under complete contact conditions. However, in such a case, even a small perturbation at the peeling front with a slight increase in s would be sufficient to cause unstable detachment. On the contrary, when χ is high the decrease of $\hat{s}_{th}$ with P/P_0 is less sharp. In such a case, given the load and starting from complete contact, initial small detachments could be tolerated without unstable propagation of the peeling front taking place. Notice the area below the curves corresponds to the region of stable adhesion, whereas above the curves unstable detachment is expected occurring.

These arguments, which are also valid for the periodic case, suggest that, in principle, we could tune the value of the elasticity ratio χ to make sufficiently high the threshold s_{th} and, as a result, to enhance the adhesive strength of the system.

4. Conclusions

In this paper, a mathematical model to study the periodic V-shaped double peeling of elastic films from soft substrates is proposed in the framework of linear elasticity. Specifically, the effect of substrate's compliance and periodically distributed multiple loads on the mechanism of peeling is investigated. An increase in the adhesion strength is found with respect to the case of rigid substrate. Such increase is due to the symmetry characterizing the geometrical configuration of the double V-peeling that determines the loss of translation invariance, which in turn makes the calculation of G sensitive to the variation of the elastic energy in the substrate.

Results show that the adhesion strength is significantly affected by the elasticity ratio χ between the Young's moduli of tape and substrate and the spatial periodicity λ. In particular, an increase in both χ and λ produces a strong enhancement of the defect tolerance of the system, i.e. initially detached lengths can be easily tolerated without causing peeling propagation and then detachment. Moreover, given the size of the initial 'defect', it is possible to arrange the contacts, by choosing the proper value of λ, in order to maximize the load per unit length which can be borne by the tape.

Acknowledgment

Appendix A. Elastic surface displacements due to periodic uniform normal and tangential stress distributions

Consider a uniform distribution of normal p and tangential q tractions acting on an elastic half-plane over a strip of size $2a = d$. Assume such tractions are periodically distributed with periodicity λ. According to Ref. (Carbone and Mangialardi, 2008), the total surface displacement vector $\mathbf{v} = (v_x, v_y)$ can be written as the convolution product between the Green's tensor $\mathbf{G}(x)$ and the interfacial stress vector $\sigma = (q, p)$

$$\mathbf{v}(x) - \mathbf{v}_m = \int_\Omega ds\, \mathbf{G}(x - s)\sigma(s); \qquad x \in [0, \lambda], \tag{A.1}$$

where Ω is the domain where the surface stresses are applied, $\mathbf{v}_m$ is the mean displacement vector and the components of the Green's tensor are given by Carbone and Mangialardi (2008)

$$G_{11}(x) = -\frac{2\left(1 - v_h^2\right)}{\pi E_h} \log \left| 2 \sin \left(\frac{kx}{2}\right)\right| \tag{A.2}$$

$$G_{21}(x) = -\frac{1 + v_h}{\pi E_h} \frac{1 - 2v_h}{2} [\mathrm{sgn}(x)\pi - kx] \tag{A.3}$$

$$G_{22}(x) = -\frac{2\left(1 - v_h^2\right)}{\pi E_h} \log \left| 2 \sin \left(\frac{kx}{2}\right)\right|, \tag{A.4}$$

where E_h and v_h are, respectively, the Young's modulus and the Poisson's ratio of the substrate material and $k = 2\pi/\lambda$. Substituting the above relations in (A.1) an after same algebraic applications, the effective normal $u_y = v_y - v_{m,y}$ and tangential $u_x = v_x - v_{m,x}$ surface displacements can be written as

$$u_y(x) = F_1(x)p - F_2(x)q \tag{A.5}$$

$$u_x(x) = F_1(x)q + F_2(x)p, \tag{A.6}$$

where the functions $F_1(x)$ and $F_2(x)$ are so defined

$$F_1(x) = -\frac{2\left(1 - v_h^2\right)}{\pi E_h} [Cl_2(x - a) - Cl_2(x + a)] \tag{A.7}$$

$$F_2(x) = -\frac{(1 - 2v_h)(1 + v_h)}{\pi E_h} [\Phi(x - a) - \Phi(x + a)] \tag{A.8}$$

being

$$Cl_2(x) = -\int_0^x \log|2 \sin(t/2)| dt \tag{A.9}$$

the Clausen function of order 2 (Ref. Abramowitz and Stegun, 1972), and

$$\Phi(x) = \frac{(kx)^2}{4} + kx \arctan [\cot(x/2)] \tag{A.10}$$

Finally, the total surface displacements are obtained by superposition of (A.5, A.6) as $\mathbf{u_{tot}}(s, x) = \mathbf{u}(x - s) + \mathbf{u}(x + s)$, being s the distance of the load distributions from the symmetry axis.

References

Abramowitz, M., Stegun, I.A.,(Eds.), 1972. Clausen's integral and related summations" section 27.8 in handbook of mathematical functions with formulas. In: Graphs, and Mathematical Tables. Dover, New York, pp. 1005–1006.

Afferrante, L., Carbone, C., 2012. Biomimetic surfaces with controlled direction-dependent adhesion. J. R. Soc. Interf. 9, 3359–3365.

Afferrante, L., Carbone, G., 2013. The mechanisms of detachment of mushroom-shaped micro-pillars: from defect propagation to membrane peeling. Macromol. React. Eng. 7, 609–615.

Afferrante, L., Carbone, G., 2016. The ultratough peeling of elastic tapes from viscoelastic substrates. J. Mech. Phys. Solids 96, 223–234.

Afferrante, L., Carbone, G., Demelio, G., Pugno, N., 2013. Adhesion of elastic thin films: double peeling of tapes versus axisymmetric peeling of membranes. Tribol. Lett. 52, 439–447.

Afferrante, L., Grimaldi, G., Demelio, G., Carbone, G., 2015. Direction-dependent adhesion of micro-walls based biomimetic adhesives. Int. J. Adhes. Adhes. 61, 93–98.

Arzt, E., Gorb, S., Spolenak, R., 2003. From micro to nano contacts in biological attachment devices. Proc. Natl. Acad. Sci. USA 100 (19), 10603–10606.

Autumn, K., Dittmore, A., Santos, D., Spenko, M., Cutkosky, M., 2006a. Frictional adhesion: a new angle on gecko attachment. J. Exp. Biol. 209, 3569–3579.

Autumn, K., Hsieh, S.T., Dudek, D.M., Chen, J., Chitaphan, C., Full, R.J., 2006b. Dynamics of geckos running vertically. J. Exp. Biol. 209, 260–272.

Autumn, K., Peattie, A.M., 2002. Mechanisms of adhesion in geckos. Int. Comput. Biol. 42, 1081–1090.

Barquins, M., Ciccotti, M., 1997. On the kinetics of peeling of an adhesive tape under a constant imposed load. Int. J. Adhes. Adhes. 17, 65–68.

Bosia, F., Colella, S., Mattoli, V., Mazzolai, B., Pugno, N.M., 2014. Hierarchical multiple peeling simulations. RSC Adv. 4 (48), 25447–25452.

Boyer, G., Lyon, C.N.R.S., Zahouani, H., Le Bot, A., Laquieze, L., 2007. In vivo characterization of viscoelastic properties of human skin using dynamic micro-indentation, engineering in medicine and biology society. In: EMBS, Twenty Nintheenth Annual International Conference of the IEEE.

Callies, X., Herscher, O., Fonteneau, C., Robert, A., Pensec, S., Bouteiller, L., Creton, C., 2016. Combined effect of chain extension and supramolecular interactions on rheological and adhesive properties of acrylic pressure-sensitive adhesives. ACS Appl. Mater. Interf. 8 (48), 33307–33315.

del Campo, A., Greiner, C., Artz, E., 2007. Contact shape controls adhesion of bioinspired fibrillar surfaces. Langmuir 23, 10235–10243.

Carbone, G., Mangialardi, L., 2004. Adhesion and friction of an elastic half-space in contact with a slightly wavy rigid surface. J. Mech. Phys. Solids 52 (6), 1267–1287.

Carbone, G., Mangialardi, L., 2008. Analysis of adhesive contact of confined layers by using a Green's function approach. J. Mech. Phy. Solids 56 (2), 684–706.

Carbone, G., Pierro, E., 2012a. Effect of interfacial air entrapment on the adhesion of bio-inspired mushroom-shaped micro-pillars. Soft Matter 8 (30), 7904–7908.

Carbone, G., Pierro, E., 2012b. Sticky bio-inspired micropillars: finding the best shape. Small 8 (9), 1449–1454.

Carbone, G., Pierro, E., Gorb, S., 2011. Origin of the superior adhesive performance of mushroom-shaped microstructured surfaces. Soft Matter 7, 5545–5552.

Carbone, G., Pierro, E., Recchia, G., 2016. Loading-unloading hysteresis loop of randomly rough adhesive contacts. Phys. Rev. E 92, 062404.

Chivers, R.A., 2001. Easy removal of pressure sensitive adhesives for skin applications. Int. J. Adhes. Adhes. 21, 381–388.

Ciavarella, M., Papangelo, A., Afferrante, L., 2017. Adhesion between self-affine rough surfaces: possible large effects in small deviations from the nominally Gaussian case. Tribol. Int. 109, 435–440.

Ciccotti, M., Giorgini, B., Vallet, D., Barquins, M., 2004. Complex dynamics in the peeling of an adhesive tape. Int. J. Adhes. Adhes. 24, 143–151.

Creton, C., Ciccotti, M., 2016. Fracture and adhesion of soft materials: a review. Rep. Prog. Phys. 79 (4), 046601.

Creton, C., Leibler, L., 1996. How does tack depend on contact time and contact pressure. J. Polym. Sci. B 34, 545–554.

Dalbe, M.-J., Santucci, S., Cortet, P.-P., Vanel, L., 2014a. Strong dynamical effects during stick-slip adhesive peeling. Soft Matter 10 (1), 132–138.

Dalbe, M.-J., Santucci, S., Vanel, L., Cortet, P.-P., 2014b. Peeling-angle dependence of the stick-slip instability during adhesive tape peeling. Soft Matter 10 (48), 9637–9643.

Dening, K., Heepe, L., Afferrante, L., Carbone, G., Gorb, S.N., 2014. Adhesion control by inflation: implications from biology to artificial attachment device. Appl. Phys. A 116 (2), 567–573.

Dies, L., Restagno, F., Weil, R., Leger, L., Poulard, C., 2015. Role of adhesion between asperities in the formation of elastic solid/solid contacts. Eur. Phys. J. E 38, 130.

Ding, J., Wen, S., Meng, Y., 2001. Theoretical study of the sticking of a membrane strip in MEMs under the Casimir effect. J. Micromech. Microeng. 11, 202–208.

Edwards, C., Marks, R., 1995. Evaluation of biomechanical properties of human skin. Clin. Dermatol. 13 (4), 375–380.

Geim, A.K., Dubonos, S.V., Grigorieva, I.V., Novoselov, K.S., Zhukov, A.A., Shapoval, S.Y., 2003. Microfabricated adhesive mimicking gecko foot-hair. Nature Mater. 2 (7), 461–463.

Glassmaker, N.J., Jagota, A., Hui, C.-Y., Noderer, W.L., Chaudhury, M.K., 2007. Biologically inspired crack trapping for enhanced adhesion. Proc. Natl. Acad. Sci. USA 104, 10786–10791.

Gravish, N., Wilkinson, M., Autumn, K., 2008. Frictional and elastic energy in gecko adhesive detachment. J. R. Soc. Interf. 6, 339–348.

Guduru, P.R., 2007. Detachment of a rigid solid from an elastic wavy surface: theory. J. Mech. Phys. Solids 55, 445–472.

Guduru, P.R., Bull, C., 2007. Detachment of a rigid solid from an elastic wavy surface - experiments. J. Mech. Phys. Solids 55, 473–488.

Huber, G., Mantz, H., Spolenak, R., Mecke, K., Jacobs, K., Gorb, S.N., Arzt, E., 2005. Evidence for capillary contributions to gecko adhesion from single spatula nanomechanical measurements. Proc. Natl. Acad. Sci. USA 102 (45), 16293–16296.

Hui, C.Y., Lin, Y.Y., aney, J.M., Kramer, J.E., 2001. The mechanics of contact and adhesion of periodically rough surfaces. J. Polym. Sci. Part B Polym. Phys. 39 (11), 1195–1214.

Hui, C.Y., Lin, Y.Y., Baney, J.M., 2000. The mechanics of tack: viscoelastic contact on a rough surface. J. Polym. Sci. Part B Poly. Phys. 38 (11), 1485–1495.

ISO 8510-1, 1990. Adhesives - peel test for a flexible-bonded-to-rigid test specimen assembly - part 1: 90° peel. ISO.

ISO 8510-2, 2006. Adhesives - peel test for a flexible-bonded-to-rigid test specimen assembly - part 2: 180° peel. ISO.

Jin, C., 2009. Theoretical study of mechanical behavior of thin circular film adhered to a flat punch. Int. J. Mech. Sci. 51, 301–313.

Johnson, K.L., Kendall, K., Roberts, A.D., 1971. Surface energy and the contact of elastic solids. Proc. R. Soc. Lond. A 324, 301–313.

Kaelble, D.H., 1959. Theory and analysis of peel adhesion: mechanisms and mechanics. Trans. Soc. Rheol. 3 (1), 161–180.

Kaelble, D.H., 1960. Theory and analysis of peel adhesion: bond stresses and distributions. Trans. Soc. Rheol. 4, 45–73.

Kaelble, D.H., 1965. Peel adhesion: micro-fracture mechanics of interfacial unbonding of polymers. Trans. Soc. Rheol. 9 (2), 135–163.

Kendall, K., 1975. Thin-film peeling-the elastic term. J. Phys. D Appl. Phys. 8, 1449–1452.

Krahn, J., Liu, Y., Sadeghi, A., Menon, C., 2011. A tailless timing belt climbing platform utilizing dry adhesives with mushroom caps. Smart Mater. Struct. 20, 115021.

Kwak, M.K., Jeong, H.-E., Suh, K.Y., 2011. Rational design and enhanced biocompatibility of a dry adhesive medical skin patch. Adv. Mater. 23, 3949–3953.

Lakrout, H., Sergot, P., Creton, C., 1999. Direct observation of cavitation and fibrillation in a probe tack experiment on model acrylic pressure-sensitive-adhesives. J. Adhes. 69 (3–4), 307–359.

Lee, J., Fearing, R.S., Komvopoulos, K., 2008. Directional adhesion of gecko-inspired angled microfiber arrays. Appl. Phys. Lett. 93 (19), 191910.

Lepore, E., Pugno, F., Pugno, N.M., 2012. Optimal angles for maximal adhesion in living tokay geckos. J. Adhes. 88 (10), 820–830.

Lin, Y.-Y., Chen, H.-Y., 2006. Effect of large deformation and material nonlinearity on the JKR (Johnson–Kendall–Roberts) test of soft elastic materials. J. Polym. Sci. Part B Polym. Phys. doi:10.1002/polb.20914.

Martina, D., Creton, C., Damman, P., et al., 2012a. Adhesion of soft viscoelastic adhesives on periodic rough surfaces. Soft Matter 8 (19), 5350–5357. doi:10.1039/c2sm07059f.

Martina, D., Creton, C., Damman, P., Jeusette, M., Lindner, A., 2012b. Adhesion of soft viscoelastic adhesives on periodic rough surfaces. Soft Matter 8, 5350.

Maugis, D., Barquins, M., 1988. Adhesion 12. Elsevier ASP, London, pp. 205–222.

Menga, N., Afferrante, L., Carbone, G., 2016a. Adhesive and adhesiveless contact mechanics of elastic layers on slightly wavy rigid substrates. Int. J Solids Struct. 88–89, 101–109.

Menga, N., Afferrante, L., Carbone, G., 2016b. Effect of thickness and boundary conditions on the behavior of viscoelastic layers in sliding contact with wavy profiles. J. Mech. Phys. Solids 95, 517–529.

Menga, N., Carbone, G., Dini, D., 2018. Do uniform tangential interfacial stresses enhance adhesion? J. Mech. Phys. Solids 112, 145–156.

Menga, N., Foti, D., Carbone, G., 2017. Viscoelastic frictional properties of rubber-layer roller bearings (RLRB) seismic isolators. Meccanica 52 (11–12), 2807–2817. doi:10.1007/s11012-016-0612-y.

Menga, N., Putignano, C., Carbone, G., Demelio, G.P., 2014. The sliding contact of a rigid wavy surface with a viscoelastic half-space. Proc. R. Soc. A 470 (20140392), 2014.

Murphy, M.P., Kute, C., Menguc, Y., Sitti, M., 2011. Waalbot II: adhesion recovery and improved performance of a climbing robot using fibrillar adhesives. Int. J. Robot. Res. 30, 118–133.

O'Rorke, R.D., Steele, T.W.J., Taylor, H.K., 2016. Bioinspired fibrillar adhesives: a review of analytical models and experimental evidence for adhesion enhancement by surface patterns. J. Adhes. Sci. Technol. 30 (4), 362–391.

Ozer, A., 2016. Mechanics of bio-inspired attachment systems contacting with rough surface: effect of spring orientation angle on hierarchical spring model. J. Adhes. Sci. Technol. 1–15.

Pereira, J.M., Mansour, J.M., Davis, B.R., 1991. Dynamic measurement of the viscoelastic properties of skin. J. Biomech. 24 (2), 157–162.

Persson, B.N.J., 2002. Adhesion between elastic bodies with randomly rough surfaces. Phys. Rev. Lett. 89, 245502.

Persson, B.N.J., 2003. On the mechanism of adhesion in biological systems. J. Chem. Phys. 118, 7614–7621.

Persson, B.N.J., Albohr, O., Creton, C., Peveri, V., 2004. Contact area between a viscoelastic solid and a hard, randomly rough, substrate. J. Chem. Phys. 120 (18), 8779–8793.

Pesika, N.S., Tian, Y., Zhao, B., Rosenberg, K., Zeng, H., McGuiggan, P., Autumn, K., Israelachvili, J.N., 2007. Peel-zone model of tape peeling based on the gecko adhesive system. J. Adhes. 83 (4), 383–401.

Pugno, N.M., 2008. Spiderman gloves. Nano Today 3 (5), 35–41.

Pugno, N.M., 2011. The theory of multiple peeling. Int. J. Fract. 171, 185–193.

Putignano, C., Afferrante, L., Mangialardi, L., Carbone, G., 2014. Equilibrium states and stability of pre-tensioned adhesive tapes. Beilstein J. Nanotechnol. 5, 1725–1731.

Rumi, D., Ananthakrishna, G., 2006. Dynamics of the peel front and the nature of acoustic emission during peeling of an adhesive tape. Phys. Rev. Lett. 97 (16), 165503.

Sekiguchi, Y., Takahashi, K., Sato, C., 2015. Adhesion mechanism of a gecko-inspired oblique structure with an adhesive tip for asymmetric detachment. J. Phys. D Appl. Phys. 48 (47), 475301.

Shanahan, M.E.R., 2000. Adhesion of a punch to a thin membrane. CR Acad. Sci. Ser. IV 1, 517–522.

Silver, F.H., Freeman, J.W., CeVoe, D., 2001. Viscoelastic properties of human skin and processed dermis. Skin Res. Technol. 7, 18–23.

Tian, Y., Pesika, N., Zeng, H.B., Rosenberg, K., Zhao, B.X., McGuiggan, P., Autumn, K., Israelachvili, J., 2006. Adhesion and friction in gecko toe attachment and detachment. Proc. Natl. Acad. Sci. USA 103 (1932), 19320–19325.

Varenberg, M., Gorb, S., 2007. Shearing of fibrillar adhesive microstructure: friction and shear-related changes in pull-off force. J. R. Soc. Interf. 4 (15), 721–725.

Varenberg, M., Pugno, N., Gorb, S., 2010. Spatulate structures in biological fibrillar adhesion. Soft Matter 6, 3269–3272.

Villey, R., Cortet, P.P., Creton, C., Ciccotti, M., 2017. In-situ measurement of the large strain response of the fibrillar debonding region during the steady peeling of pressure sensitive adhesives. Int. J. Fract. 204, 175–190.

Villey, R., Creton, C., Cortet, P.P., Dalbe, M.J., Jet, T., Saintyves, B., Ciccotti, M., 2015. Rate-dependent elastic hysteresis during the peeling of pressure sensitive adhesives. Soft Matter 11 (17), 3480–3491.

Wan, K.T., 2001. Adherence of an axisymmetric flat punch on a flexible membrane. J. Adhes. 75, 369–380.

Wolff, J.O., Grawe, I., Wirth, M., Karstedt, A., Gorb, S.N., 2015. Spider's super-glue: thread anchors are composite adhesives with synergistic hierarchical organization. Soft Matter 11 (12), 2394–2403.

Wu, J.-J., 2012. Numerical simulation of the adhesive contact between a slightly wavy surface and a half-space. J. Adhes. Sci. Technol. 26, 331–351.